^{18}F-FEDAC as a Targeting Agent for Activated Macrophages in DBA/1 Mice with Collagen-Induced Arthritis: Comparison with ^{18}F-FDG

Seock-Jin Chung*[1–3], Hai-Jeon Yoon*[1,4], Hyewon Youn[1,3,5,6], Mi Jeong Kim[1,3], Yun-Sang Lee[1,7], Jae Min Jeong[1,7,8], June-Key Chung[1–3,5,7,8], Keon Wook Kang[1–3,6,7,8], Lin Xie[9], Ming-Rong Zhang[9], and Gi Jeong Cheon[1–3,7]

[1]Department of Nuclear Medicine, Seoul National University College of Medicine, Seoul, Korea; [2]Tumor Biology Program, Seoul National University College of Medicine, Seoul, Korea; [3]Cancer Research Institute, Seoul National University College of Medicine, Seoul, Korea; [4]Department of Nuclear Medicine, College of Medicine, Ewha Womans University, Seoul, Korea; [5]Tumor Microenvironment Global Core Research Center, Seoul National University College of Medicine, Seoul, Korea; [6]Cancer Imaging Center, Seoul National University Hospital, Seoul, Korea; [7]Institute of Radiation Medicine, Medical Research Center, Seoul National University College of Medicine, Seoul, Korea; [8]Biomedical Sciences, Seoul National University College of Medicine, Seoul, Korea; and [9]Department of Radiopharmaceutical Development, National Institute of Radiological Sciences, National Institutes for Quantum and Radiological Science and Technology, Chiba, Japan

Activated macrophages have been known to play pivotal roles in the pathogenesis of rheumatoid arthritis (RA). ^{18}F-FEDAC (*N*-benzyl-*N*-methyl-2-[7,8-dihydro-7-(2-^{18}F-fluoroethyl)-8-oxo-2-phenyl-9*H*-purin-9-yl]acetamide) is a radiolabeled ligand for the 18-kDa translocator protein (TSPO), which is abundant in activated macrophages. We evaluated the feasibility of using ^{18}F-FEDAC in a murine RA model. **Methods:** RAW 264.7 mouse macrophages were activated by lipopolysaccharide. TSPO expression levels in activated and inactivated macrophages were measured by quantitative polymerase chain reaction and Western blotting. The cellular uptake and specific binding of ^{18}F-FEDAC were measured using a γ-counter. For the in vivo study, collagen-induced arthritis (CIA) was developed in DBA/1 mice, and the clinical score for arthritis was measured regularly. ^{18}F-FEDAC and ^{18}F-FDG PET images were acquired on days 23 and 37 after the first immunization. Histologic examinations were performed to evaluate macrophages and TSPO expression. **Results:** We found increased TSPO messenger RNA and protein expression in activated macrophages. Uptake of ^{18}F-FEDAC in activated macrophages was higher than that in nonactivated cells and was successfully blocked by the competitor, PK11195. In CIA mice, joint swelling was apparent on day 26 after the first immunization, and the condition worsened by day 37. ^{18}F-FEDAC uptake by arthritic joints increased early on (day 23), whereas ^{18}F-FDG uptake did not. However, ^{18}F-FDG uptake by arthritic joints markedly increased at later stages (day 37) to a higher level than ^{18}F-FEDAC uptake. The ^{18}F-FEDAC uptake correlated weakly with summed severity score ($P = 0.019$, $r = 0.313$), whereas the ^{18}F-FDG uptake correlated strongly with summed severity score ($P < 0.001$, $r = 0.897$). Histologic sections of arthritic joints demonstrated an influx of macrophages compared with that in normal joints. **Conclusion:** ^{18}F-FEDAC enabled the visualization of active inflammation sites in arthritic joints in a CIA model by targeting TSPO expression in activated macrophages. The results suggest the potential usefulness of ^{18}F-FEDAC imaging in the early phase of RA.

Received Aug. 11, 2017; revision accepted Dec. 13, 2017.
For correspondence or reprints contact: Gi Jeong Cheon, Seoul National University College of Medicine, 101 Daehak-ro, Chongno-gu Seoul 110-744, Korea.
E-mail: larrycheon@gmail.com
*Contributed equally to this work.
Published online Jan. 11, 2018.

Key Words: ^{18}F-FEDAC; TSPO; activated macrophage; rheumatoid arthritis; ^{18}F-FDG

J Nucl Med 2018; 59:839–845
DOI: 10.2967/jnumed.117.200667

Rheumatoid arthritis (RA) is a common autoimmune disease characterized by chronic synovial inflammation, which ultimately leads to joint deformity and dysfunction (*1*). Once the immune system is triggered by genetic and environmental factors, subclinical inflammation is induced by activation of T cells, B cells, and macrophages. After this, symptoms related with RA are detectable and clinical diagnoses can be made.

Current imaging modalities for diagnosis and monitoring of RA are confined exclusively to the anatomic level. Radiography and CT effectively help visualize morphologic changes such as articular bony erosion or joint space narrowing. However, such changes cannot be reliably detected earlier than 6–12 mo after RA onset. Ultrasonography, MRI, and ^{99m}Tc-disphosphonate SPECT help visualize abnormal findings in the early stages of RA; however, they are still limited by a lack of specificity regarding inflammation (*2–6*).

^{18}F-FDG PET has been clinically used for tumor imaging, because glucose metabolism increases in cancer cells. Recently, use of ^{18}F-FDG PET has expanded for inflammatory diseases, including RA, because glucose metabolism also increases in neutrophils and activated macrophages; however, ^{18}F-FDG has limited value in subclinical inflammation (*7–11*).

Besides ^{18}F-FDG, more specific PET tracers based on RA pathogenesis have been developed. Activated macrophages are central effectors of synovial inflammation in early stages of RA and release proinflammatory cytokines, including tumor necrosis factor-α, interleukin-1, and interleukin-6 (*1,12,13*). Therefore, targeting and visualization of macrophages in subclinically inflamed synovium enable earlier diagnosis and therapeutic intervention.

The 18-kDa translocator protein (TSPO) is overexpressed in activated macrophages (*14–17*). ^{11}C-PK11195 ((*R*)-*N*-methyl-*N*-(1-methylpropyl)-1-(2-chlorophenyl)-isoquinoline-3-carboxamide) is a prototypical radioligand for PET imaging and has recently been applied to the study of RA (*17*). However, its clinical applications are limited by a relatively low specific-to-nonspecific uptake ratio, high plasma protein binding, very high lipophilicity, and considerable periarticular background activity (*15*). ^{18}F-FEDAC (*N*-benzyl-*N*-methyl-2-[7,8-dihydro-7-(2-^{18}F-fluoroethyl)-8-oxo-2-phenyl-9*H*-purin-9-yl]acetamide) is a second-generation TSPO ligand with high selectivity. The feasibility of using ^{18}F-FEDAC for RA research has not been studied, although it has been used to study neuroinflammation, brain infarction, and lung inflammation models by reflecting increased TSPO expression (*18–20*).

The aim of the present study was to apply the new TSPO radioligand ^{18}F-FEDAC to visualize synovial inflammation associated with RA. We performed in vitro assays and in vivo PET to evaluate TSPO expression in activated macrophage and inflamed joints of collagen-induced arthritis (CIA) models. In addition, for the detection of subclinical arthritis, we evaluated the value of ^{18}F-FEDAC compared with ^{18}F-FDG, which is the most widely used radioligand for inflammation via glucose metabolism of diverse inflammatory cells.

MATERIALS AND METHODS

Synthesis of ^{18}F-FEDAC

^{18}F-fluoride was produced in-house using a cyclotron (PETtrace; GE Healthcare) and captured on a Chromafix cartridge (PS-HCO3; ABX), which was preconditioned using ethanol (1 mL) and water (1 mL). ^{18}F-fluoride on the cartridge was eluted into a reaction vial containing a mixture (1 mL) of acetonitrile (83.8%) and tetrabutylammonium bicarbonate (2.3%). Two azeotropic evaporations were conducted at 110°C, after the addition of 1 mL of acetonitrile each time, under a gentle stream of nitrogen gas. The precursor of ^{18}F-FEDAC, TosOEt-DAC (*N*-benzyl-*N*-methyl-2-[7,8-dihydro-7-(2-tosyloxyethyl)-8-oxo-2-phenyl-9*H*-purin-9-yl]acetamide, 1.3 mg), in dimethylformamide (0.6 mL) was added to the reaction vial and heated to 95°C for 15 min. The reaction mixture was diluted using 40% EtOH and subjected to semipreparative high-performance liquid chromatography (Xterra Prep RP18, 10 μm, 10 × 250 mm; 40% EtOH for 20 min; 5 mL/min; Waters). The radiochemical purity was more than 99% on analytic high-performance liquid chromatography (Xterra RP18, 10 μm, 4.6 × 100 mm; 40% EtOH for 20 min, 1 mL/min; Waters), and the radiochemical yield of ^{18}F-FEDAC was 24.8% ± 1.4% in a total synthesis time of 50 min. The specific activity of ^{18}F-FEDAC was 265.1 ± 93.1 GBq/μmol (n = 3) (*21*). All the technical support for radiosynthesis, including the precursor and cold standard of ^{18}F-FEDAC, was kindly provided by Lin Xie and Ming-Rong Zhang (National Institute of Radiologic Sciences and National Institutes for Quantum and Radiologic Science and Technology, Chiba, Japan).

Cell Culture

The mouse macrophage cell line RAW 264.7 was obtained from the American Type Culture Collection. RAW 264.7 cells were grown using Dulbecco modified Eagle medium (WelGene Inc.) supplemented with 10% fetal bovine serum (Invitrogen) and 1% antibiotics (Invitrogen) at 37°C in a humidified atmosphere containing 5% CO_2. For activation, RAW 264.7 cells were treated with a 1 μg/mL concentration of lipopolysaccharide (Sigma-Aldrich) for 24 h (*22*).

In Vitro Real-Time Polymerase Chain Reaction (PCR) Analysis and Western Blot Analysis

Total RNA was extracted from cells using TRIzol reagent (Invitrogen) and converted into complementary DNA using a complementary DNA synthesis kit (GenDEPOT). TSPO in macrophages was quantified using SYBR Green real-time PCR Master Mix (TaKaRa) with 2 ng of complementary DNA and 0.2 μM primers. Expression of the housekeeping gene 18S rRNA was used to standardize TSPO expression. Real-time PCR was performed using an Applied Biosystems 7500 Sequence Detection System instrument with the following parameters: 50°C for 2 min, 95°C for 10 min, and 40 cycles of 95°C for 15 s and 60°C for 1 min.

Total protein was isolated from the cells using radioimmunoprecipitation assay buffer (Sigma-Aldrich). The lysate of each sample was loaded onto NuPAGE 4%–12% Bis-Tris Gel (Invitrogen). After electrophoresis, the gels were blotted onto polyvinylidene difluoride membranes (Millipore), which were subsequently blocked with 5% skim milk for 1 h at room temperature. The membranes were incubated overnight at 4°C with primary antibodies targeting TSPO (Abcam; diluted 1:10,000) and β-actin (Sigma-Aldrich; diluted 1:5,000). Membranes were then probed with horseradish peroxidase–conjugated antirabbit or antimouse IgG (Cell Signaling Technology). The signal intensity was measured using an LAS-3000 imaging system (Fujifilm).

In Vitro Cellular Uptake of TSPO Radioligand

^{18}F-FEDAC uptake in vitro was examined using a 0.37–55.5 kBq/mL concentration of ^{18}F-FEDAC in assay medium (Hanks balanced salt

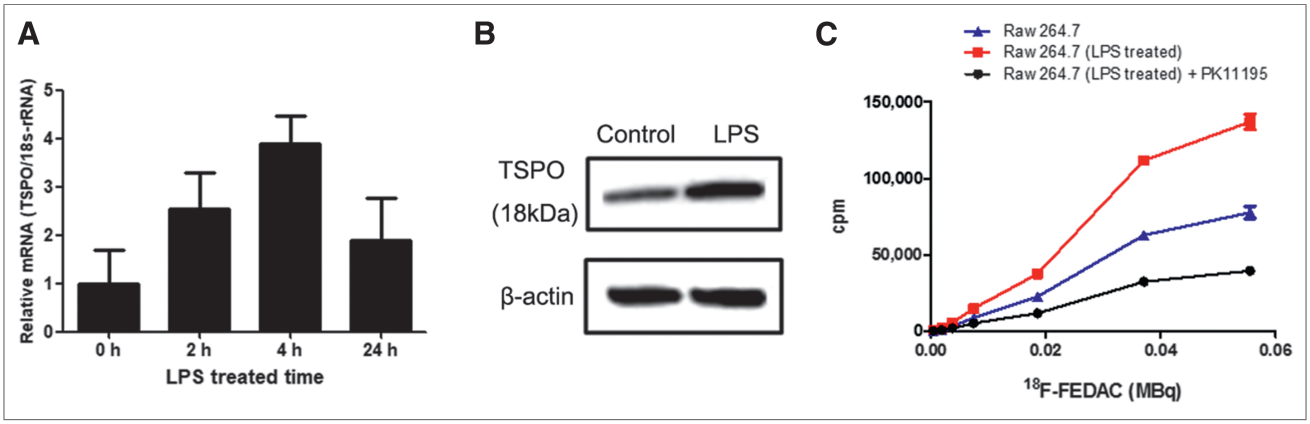

FIGURE 1. (A) Time-dependent TSPO messenger RNA level after lipopolysaccharide (LPS) stimulation. (B) TSPO protein level after 24-h stimulation. (C) Dose-dependent ^{18}F-FEDAC uptake of RAW 264.7 cells (blue). Stimulation for 24 h enhanced ^{18}F-FEDAC uptake (red), whereas cold-form PK11195 blocked ^{18}F-FEDAC uptake (black).

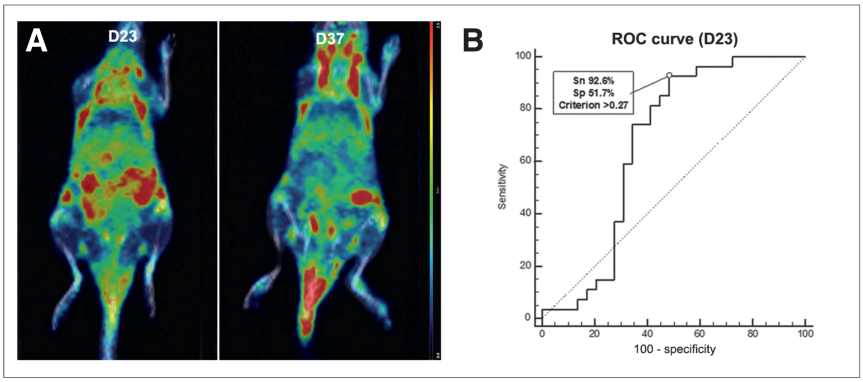

FIGURE 2. (A) Coronal ^{18}F-FEDAC PET/CT section of same CIA mouse on days 23 and 37, showing increased uptake in front and hind paws. (B) Predictive performance of day 23 ^{18}F-FEDAC uptake for development of clinical arthritis. ROC = receiver operating characteristic; Sn = sensitivity; Sp = specificity.

solution, 0.5% bovine serum albumin [w/v], 0.24% 4-(2-hydroxyethyl)-1-piperazineethanesulfonic acid [w/v], pH 7.4). Incubation was performed for 1 h at room temperature based on the pretest results (Supplemental Fig. 1; supplemental materials are available at http://jnm.snmjournals.org). RAW 264.7 cells were incubated in culture medium with or without lipopolysaccharide stimulation for 24 h, and the culture medium was then replaced with 1 mL of assay medium. After incubation with ^{18}F-FEDAC, uptake was terminated by 2 washes using cold phosphate-buffered saline. Then, the cells were solubilized with 500 μL of 1% sodium dodecyl sulfate buffer. The radioactivity of the nonactivated control and the activated macrophages was measured using a γ-counter (PerkinElmer). The uptake of ^{18}F-FEDAC was calculated from the ratio of ^{18}F-FEDAC associated with the cells to the initial dose. To verify in vitro specific TSPO binding of ^{18}F-FEDAC, an excess of cold-form PK11195 (1,000-fold molar excess) was used to compete with ^{18}F-FEDAC.

Induction and Assessment of CIA Mouse Model

All experimental procedures were approved by the Institutional Animal Care and Use Committee of the Seoul National University Hospital. All specific pathogen-free male DBA/1 (22.8 ± 2.5 g, 6-wk-old) mice were purchased from Japan SLC Inc. The CIA mouse model was induced as described previously (*23*). Bovine type II collagen (Chondrex, Inc.) dissolved in 0.1 M acetic acid was emulsified with an equal volume of complete Freund adjuvant and then injected subcutaneously at the base of the tail (50 μL per mouse). Three weeks after the first immunization, type II collagen emulsified with incomplete Freund adjuvant was injected subcutaneously as a booster immunization (50 μL per mouse).

From the day of the second immunization, the mice were clinically examined every 2 d. The clinical severity scoring of arthritis in the paw was performed as described previously (*23*): score 0, no macroscopic evidence of erythema or swelling; score 1, erythema and mild swelling confined to the tarsals; score 2, erythema and mild swelling extending from the ankle to the tarsals; score 3, erythema and moderate swelling extending from the ankle to the tarsals; and score 4, erythema and severe swelling encompassing the ankle, foot, and digits, or ankylosis of the limb. To obtain the summed severity score per animal, the results from all paws of that animal were added.

^{18}F-FEDAC and ^{18}F-FDG PET Imaging

PET was performed using a small-animal PET/CT scanner (eXplore Vista; GE Healthcare). We measured ^{18}F-FEDAC uptake in all paws of mice with CIA (n = 10) at 2 different time points of disease (days 23 and 37) and compared it with the uptake of the control group (n = 4). We measured ^{18}F-FDG uptake in all paws of mice with CIA (n = 5) at 2 different time points of disease (days 23 and 37) and compared it with the uptake of the control group (n = 2).

The mice were anesthetized with 1.5% isoflurane, and the radiotracers were intravenously injected (8.7 ± 0.1 MBq/100 μL for ^{18}F-FEDAC; 9.5 ± 0.7 MBq/100 μL for ^{18}F-FDG). PET/CT images were acquired 2 and 1 h after injection of ^{18}F-FEDAC and ^{18}F-FDG, respectively. Images were reconstructed using a 3-dimensional ordered-subset expectation maximization algorithm. To verify specific TSPO binding, CIA mice were pretreated with a more than 1,000-fold molar excess of the nonradioactive PK11195 before the injection of ^{18}F-FEDAC and followed by PET imaging.

PET Image Analysis

Quantitative analysis was performed by an experienced nuclear medicine physician using PMOD software, version 3.3. The SUV_{max} was measured by placing a 3-dimensional volume of interest encasing each paw with a margin threshold set as 40% SUV_{max}. The SUV in a pixel was calculated as tissue radioactivity concentration/(injected radioactivity/body weight). Next, the SUV_{max} of the paw was divided by the blood-pool SUV_{max} measured from the aorta for normalization. Finally, after these calculations, a target-to-background ratio (TBR) was acquired.

Histopathology and Immunostaining

The paws were amputated and fixed in 10% paraformaldehyde for 7 d at 4°C. Bone tissue was decalcified for about 1 wk at 4°C in a solution with 14% ethylenediaminetetraacetic acid (pH 7.2; Sigma-Aldrich). After decalcification, the joints were washed and prepared for paraffin embedding. Sagittal sections (4 μm) from the center of the joint were used for staining. The sections were stained with hematoxylin and eosin for histologic evaluation.

Immunofluorescence staining of the macrophages was performed using anti-CD68 antibody (diluted 1:100; Abcam), and TSPO receptor staining was performed using anti-TSPO antibody (diluted 1:400; Abcam) incubated overnight at 4°C. After washing with phosphate-buffered

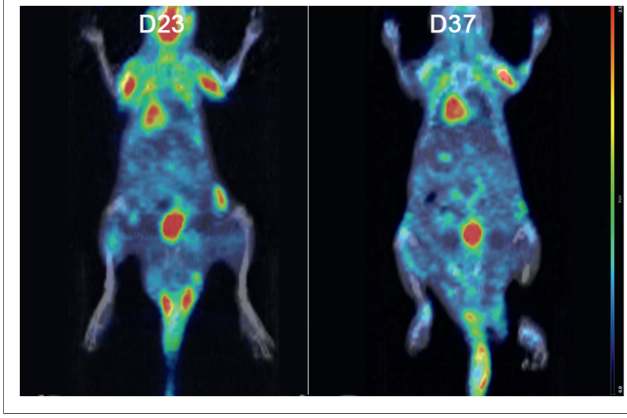

FIGURE 3. Coronal ^{18}F-FDG PET/CT section of same mouse on days 23 and 37. On day 23, before onset of arthritis, uptake by joints was not observed. On day 37, increased ^{18}F-FDG uptake was observed for all 4 arthritic joints.

TABLE 1
TBR in Normal and CIA Mice

Tracer	Day 23			Day 37			*P* for day 23 vs. 37*
	Normal	CIA	*P*	Normal	CIA	*P*	
^{18}F-FEDAC	0.22 ± 0.04	0.50 ± 0.16	<0.001†	0.18 ± 0.06	0.49 ± 0.27	<0.001†	0.183
^{18}F-FDG	0.17 ± 0.07	0.17 ± 0.05	0.838	0.28 ± 0.07	0.62 ± 0.27	<0.001†	<0.001†

*Time serial comparison of uptake in CIA group.
†Statistically significant.

saline, Alexa 488– and Alexa 647–conjugated secondary antibodies were incubated for 1 h at room temperature. After staining, the slides were mounted using Prolong Gold reagent with 4′,6-diamidino-2-phenylindole (Invitrogen). Fluorescence images were obtained using an LSM 800 confocal imaging system (Carl Zeiss).

Statistics

All statistical analyses were performed using MedCalc software. Mann–Whitney tests were performed to analyze differences in PET uptake between arthritic joints of CIA mice and normal joints of control mice. Kruskal–Wallis testing was performed to evaluate the PET uptake according to the clinical severity score. The clinical severity score was reclassified as 3 grades by merging scores 2–4, for which arthritis extended from the ankle to the tarsals (score 0, grade 0; score 1, grade 1; scores 2–4, grade 2), and then was referred for further statistical analysis. Rank correlation testing was performed to evaluate the relationship of PET uptake with summed severity score. A Wilcoxon signed rank test was performed for paired observations, such as nonblocking versus blocking subjects. *P* values of less than 0.05 were regarded as statistically significant. In addition, receiver-operating-characteristic curves were used to evaluate the predictive performance of PET uptake for the development of clinical arthritis. The optimal cutoff—the point that has the maximal sum of sensitivity and specificity—was determined using the Youden index.

RESULTS

Expression Level of TSPO in Activated Macrophages

After 24 h of lipopolysaccharide stimulation, RAW 264.7 cells were activated, as observed under a microscope (Supplemental Fig. 2). Real-time PCR demonstrated increased RNA expression of TSPO in activated macrophages compared with nonactivated controls (Fig. 1A). Western blot analysis demonstrated greater TSPO protein expression in activated macrophages than in nonactivated controls (Fig. 1B).

In Vitro Cell Uptake and Specific Binding of ^{18}F-FEDAC in Activated Macrophages

Uptake of ^{18}F-FEDAC in activated macrophage was higher than that in nonactivated controls (Fig. 1C). In addition, specific TSPO binding of ^{18}F-FEDAC was demonstrated, and an approximately 0.3-fold decrease in ^{18}F-FEDAC uptake was observed in activated macrophages by the specific competitor, PK11195.

Clinical Course of CIA

Among the 26 mice used for CIA modeling, 24 successfully developed clinical arthritis (92.3%). Joint swelling was apparent on day 26 after the first immunization (day 0), and the condition worsened by day 37 (Supplemental Fig. 3).

PET Imaging Analysis

Quantification of Joint Inflammation Using ^{18}F-FEDAC and ^{18}F-FDG PET/CT. Joint uptake of ^{18}F-FEDAC in CIA mice was observed on day 23 but did not increase by day 37. The TBR in CIA mice was significantly higher than that in the control group on day 23 ($P < 0.001$, Supplemental Figs. 4A–4C and Fig. 2A), although no CIA mice developed clinical arthritis. On day 37, all CIA mice developed clinical arthritis, and the TBR in CIA mice was still higher than that in control mice ($P < 0.001$, Supplemental Figs. 4D–4F and Fig. 2A). Despite the deterioration

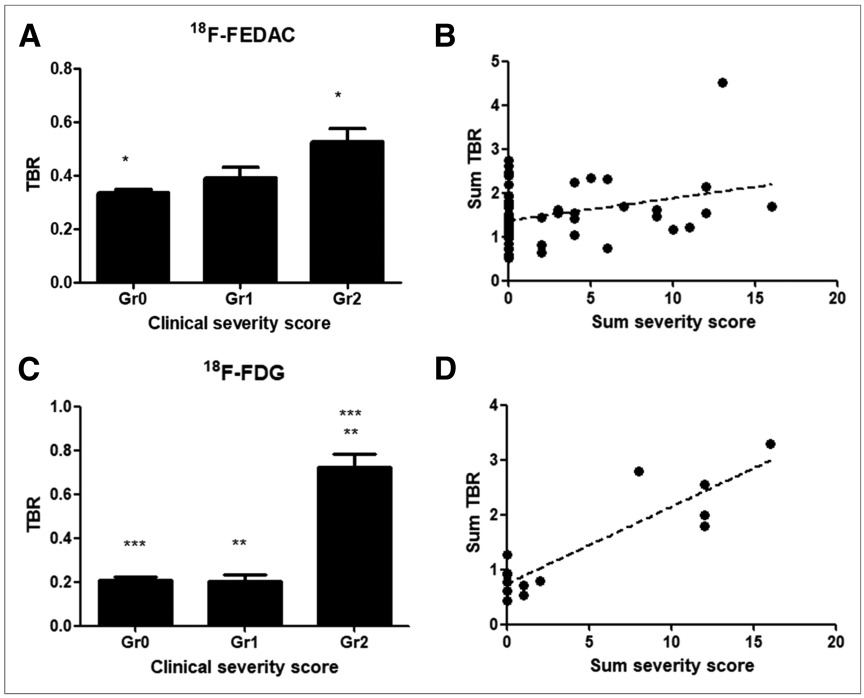

FIGURE 4. (A and C) ^{18}F-FEDAC and ^{18}F-FDG uptake according to clinical severity score (grade 0 = score 0, grade 1 = score 1, grade 2 = scores 2–4). (B and D) Scatterplot of summed ^{18}F-FEDAC and ^{18}F-FDG uptake by summed severity score (sum of all scores in mouse).

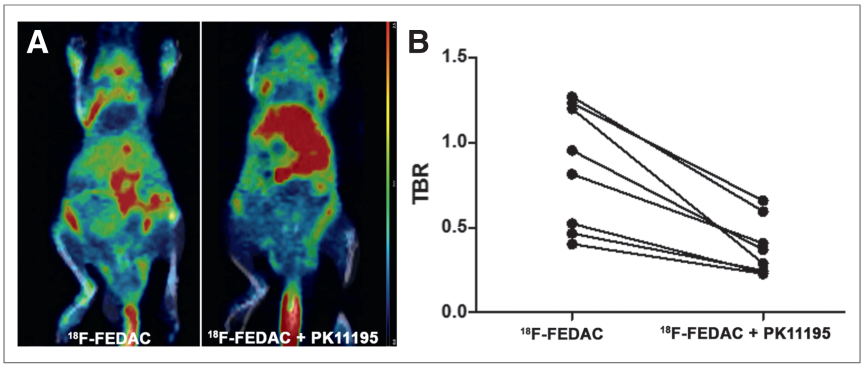

FIGURE 5. Coronal PET/CT section (A) and graph (B) before and after blocking in same mouse. ^{18}F-FEDAC uptake in arthritic joint was significantly decreased after blockade.

of clinical arthritis as compared with that on day 23, the TBR in CIA mice on day 37 was no different from ^{18}F-FEDAC uptake on day 23 ($P = 0.183$, Supplemental Figs. 4G–4I).

Joint uptake of ^{18}F-FDG in CIA mice was detected only on day 37. The TBR in CIA mice was not significantly different from that in control mice on day 23 ($P = 0.838$, Supplemental Figs. 5A–5C and Fig. 3). On day 37, all CIA mice showed prominent signs of clinical arthritis, and the TBR in CIA mice was significantly higher than that in control mice ($P < 0.001$, Supplemental Figs. 5D–5F and Fig. 3). With deterioration of clinical arthritis, the TBR in CIA mice on day 37 was significantly higher than that on day 23 ($P < 0.001$, Supplemental Figs. 5G–5I). Detailed data for ^{18}F-FEDAC and ^{18}F-FDG are summarized in Table 1.

Relationship of Clinical Score with ^{18}F-FEDAC and ^{18}F-FDG Uptake. The appearance and severity of arthritis, and the ^{18}F-FEDAC uptake in each paw, differed for each mouse (Supplemental Fig. 6). The ^{18}F-FEDAC TBR of each paw was significantly different according to the associated clinical severity score ($P < 0.001$, Fig. 4A). The total ^{18}F-FEDAC TBR of all paws from PET imaging correlated weakly with the summed severity score ($P = 0.019$, $r = 0.313$, Fig. 4B). The ^{18}F-FDG TBR of each arthritic paw was significantly different according to the clinical severity score ($P < 0.001$, Fig. 4C). The total ^{18}F-FDG TBR of all paws from PET imaging correlated strongly with the summed severity score ($P < 0.001$, $r = 0.897$, Fig. 4D). The correlation between ^{18}F-FDG TBR and the summed severity score was significantly stronger than the correlation between ^{18}F-FEDAC TBR and the summed severity score ($P < 0.001$).

Predictive Performance of ^{18}F-FEDAC Uptake on Day 23 for Development of Clinical Arthritis. Although arthritis was not detected in CIA mice on day 23, the ^{18}F-FEDAC TBR was significantly higher than that in control mice. Such a result indicates the potential of ^{18}F-FEDAC TBR to reflect subclinical inflammation. Thus, we evaluated the predictive performance of ^{18}F-FEDAC on day 23 for the development of clinical arthritis by receiver-operating-characteristic curve analyses (Fig. 2B). The optimal cutoff was 0.27 (area under the curve, 0.668; $P = 0.031$), and ^{18}F-FEDAC uptake on day 23 predicted the development of clinical arthritis with a sensitivity of 92.6% and a specificity of 51.7%.

Specific Binding of ^{18}F-FEDAC in CIA Model. We confirmed specific ^{18}F-FEDAC binding on inflammatory joints in CIA mice. After blocking of TSPO with an excess of PK11195, arthritic joint uptake of ^{18}F-FEDAC was significantly decreased compared with uptake in joints with nonblocked TSPO ($P = 0.007$, Fig. 5).

Presence of Activated Macrophages in Arthritic Paws

Hematoxylin and eosin staining of the arthritic joints of CIA mice showed a massive infiltration of mainly polymorphonuclear cells in hyperplastic synovium, with pannus formation and bone destruction (Fig. 6). Immunofluorescence staining demonstrated a prominent influx of macrophages characterized by CD68-positive and TSPO-positive cells at the inflammation site (Fig. 7). Staining specificity was verified using a negative control (Supplemental Fig. 7).

DISCUSSION

In this study, the increase of TSPO expression corresponded to the increase of ^{18}F-FEDAC uptake in activated macrophages. Real-time PCR and Western blotting revealed higher TSPO messenger RNA and protein expression in activated macrophages than in resting macrophages. Histologic sections of arthritic joints demonstrated an increase in macrophage infiltration and TSPO expression. Upregulation of TSPO in activated macrophages has been reported previously and corresponds with our data (*20,24,25*). An increase of ^{18}F-FEDAC uptake in lipopolysaccharide-stimulated macrophage cells and arthritic joints was demonstrated, indicating a corresponding overexpression of TSPO. The specific binding of ^{18}F-FEDAC to TSPO was identified by an in vitro and in vivo blocking study.

We investigated time-dependent uptake of ^{18}F-FEDAC compared with ^{18}F-FDG using CIA mice. Among several RA models, the CIA model has been the most widely investigated, and it has been reported that the first signs of arthritis are visually detectable between 21 and 28 d after immunization (*23*). Here, the first sign of joint swelling was detected on day 26, and swelling

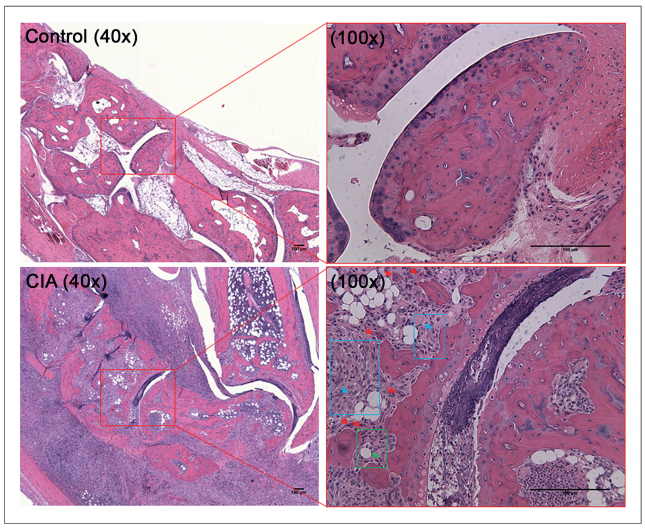

FIGURE 6. Hematoxylin- and eosin-stained sections from control and CIA joints. In control joint, synovial membrane and cartilage are intact. In CIA joint at ×100 magnification, influx of macrophages (regions in blue boxes) and neutrophils (region in green box) are prominent. Subset of osteoclasts (red arrows) indicates joint destruction. Blue arrows indicate individual macrophages (representative ones) in macrophage influx site (blue box). Green arrows indicate individual neutrophils (representative ones) in neutrophil influx site (green box).

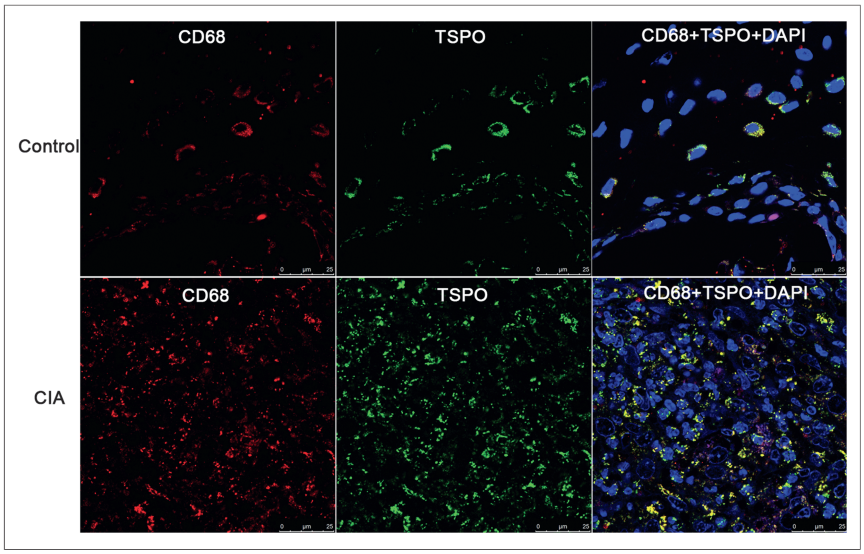

FIGURE 7. Immunofluorescence staining for CD68 (red) and TSPO (green) in synovium of control and CIA joints. Merged images at far right show increased number and TSPO expression of CD68-positive macrophages, compared with controls.

gradually increased until day 37. On the basis of previous and current results regarding the clinical course of CIA models, we selected days 23 and 37 as the early and late time points, respectively, for arthritis.

^{18}F-FEDAC uptake increased in the joints of CIA mice on day 23, although no CIA mouse developed signs of clinical arthritis. With a cutoff of 0.27, ^{18}F-FEDAC uptake on day 23 can predict the development of clinical arthritis with a sensitivity of 92.6%. From days 23 to 37, ^{18}F-FEDAC uptake did not increase and remained constant despite the deterioration of clinical arthritis. The serial uptake pattern of ^{18}F-FEDAC, which can be described as an early increase–late plateau, indicated that TSPO expression in activated macrophages at the inflammation site increased during the early stage. However, TSPO levels may be considerably low in the late phase, despite macrophage proliferation and recruitment during RA progression.

Unlike ^{18}F-FEDAC, ^{18}F-FDG uptake did not increase in the joints of CIA mice on day 23. Therefore, ^{18}F-FDG has limited use in early RA detection. On day 37, ^{18}F-FDG uptake increased along with the deterioration of clinical arthritis. The serial uptake pattern of ^{18}F-FDG, which can be described as a time-dependent increase, indicated that diverse inflammatory cells congregate in the inflammation site at later stages of RA, which induces an increase in ^{18}F-FDG uptake. Previous studies also reported no ^{18}F-FDG uptake in subclinical arthritis, whereas increased ^{18}F-FDG uptake in the acute and chronic stages was detected (*7,26*).

Therefore, we speculate that compared with ^{18}F-FDG, ^{18}F-FEDAC is a more applicable radiotracer for early detection of RA. Although the precise function of TSPO is not known, it may be involved in the initiation of autoimmune arthritis. Temporal TSPO expression during the early and late phases should be analyzed using arthritic postmortem joint tissues. Moreover, validating the potential of ^{18}F-FEDAC as a therapeutic indicator for therapies targeting macrophages or macrophage-related cytokines will be useful.

In addition, we investigated the uptake of ^{18}F-FEDAC and ^{18}F-FDG based on the clinical severity of arthritis. Although ^{18}F-FDG has a limited use in subclinical arthritis, its uptake in arthritic joints has been reported to reflect disease activity (*9,11*). Similar to previous studies, we also observed a strong correlation between ^{18}F-FDG and disease severity. This correlation was stronger than that observed for ^{18}F-FEDAC. Therefore, ^{18}F-FDG is a valuable tool for evaluation of disease severity and therapeutic responses during late RA stages.

A limitation of this study was that we could not perform a head-to-head comparison between ^{18}F-FEDAC and ^{18}F-FDG PET scans in the same mouse at the same time, because of the long half-life of ^{18}F. Although PET scans were performed for different mice, CIA was induced under the same conditions, and the course and severity of arthritis between the ^{18}F-FEDAC and ^{18}F-FDG groups were similar. Simultaneous use of the ^{11}C-labeled TSPO ligand and ^{18}F-FDG can be considered for head-to-head comparison at the same time during the development of arthritis. Especially, ^{11}C-PBR28 has been proven to have a higher binding affinity for TSPO than PK11195 (*27*). A head-to-head comparison between ^{18}F-FEDAC and ^{11}C-PBR28 with cold-form PBR28 blocking might also be considered to confirm the specificity of the tracer in the CIA model.

CONCLUSION

^{18}F-FEDAC can be used to visualize active inflammation in arthritic joints in a CIA mouse model by targeting TSPO expression in activated macrophages, which is the major effector of RA pathogenesis. The results of this study suggest the potential usefulness of ^{18}F-FEDAC imaging in early stages of RA.

DISCLOSURE

This study was supported by a grant from the Korea Health Technology R&D Project through the Korea Health Industry Development Institute (KHIDI), funded by the Ministry of Health & Welfare, Republic of Korea to Gi Jeong Cheon (grant HI14C1072), by a grant from the National Research Foundation to Hai-Jeon Yoon (2015R1C1A2A01054113) and to Keon Wook Kang (2015M3D6A1065663), and by a grant from the Global Core Research Center (GCRC) (no. 2011-0030001) to June-Key Chung. No other potential conflict of interest relevant to this article was reported.

REFERENCES

1. McInnes IB, Schett G. The pathogenesis of rheumatoid arthritis. *N Engl J Med.* 2011;365:2205–2219.
2. Wunder A, Straub RH, Gay S, Funk J, Muller-Ladner U. Molecular imaging: novel tools in visualizing rheumatoid arthritis. *Rheumatology.* 2005;44:1341–1349.
3. Taylor PC. The value of sensitive imaging modalities in rheumatoid arthritis. *Arthritis Res Ther.* 2003;5:210–213.
4. Peterfy CG. New developments in imaging in rheumatoid arthritis. *Curr Opin Rheumatol.* 2003;15:288–295.
5. Hoving JL, Buchbinder R, Hall S, et al. A comparison of magnetic resonance imaging, sonography, and radiography of the hand in patients with early rheumatoid arthritis. *J Rheumatol.* 2004;31:663–675.

6. Buchbender C, Ostendorf B, Mattes-György K, et al. Synovitis and bone inflammation in early rheumatoid arthritis: high-resolution multi-pinhole SPECT versus MRI. *Diagn Interv Radiol.* 2013;19:20–24.
7. Irmler IM, Opfermann T, Gebhardt P, et al. In vivo molecular imaging of experimental joint inflammation by combined ^{18}F-FDG positron emission tomography and computed tomography. *Arthritis Res Ther.* 2010;12:R203.
8. Matsui T, Nakata N, Nagai S, et al. Inflammatory cytokines and hypoxia contribute to ^{18}F-FDG uptake by cells involved in pannus formation in rheumatoid arthritis. *J Nucl Med.* 2009;50:920–926.
9. Wang SC, Xie Q, Lv WF. Positron emission tomography/computed tomography imaging and rheumatoid arthritis. *Int J Rheum Dis.* 2014;17:248–255.
10. Ju JH, Kang KY, Kim IJ, et al. Visualization and localization of rheumatoid knee synovitis with FDG-PET/CT images. *Clin Rheumatol.* 2008;27(suppl 2):S39–S41.
11. Beckers C, Ribbens C, Andre B, et al. Assessment of disease activity in rheumatoid arthritis with ^{18}F-FDG PET. *J Nucl Med.* 2004;45:956–964.
12. Kinne RW, Brauer R, Stuhlmuller B, Palombo-Kinne E, Burmester G-R. Macrophages in rheumatoid arthritis. *Arthritis Res.* 2000;2:189–202.
13. Ma Y, Pope RM. The role of macrophages in rheumatoid arthritis. *Curr Pharm Des.* 2005;11:569–580.
14. Folkersma H, Foster Dingley JC, van Berckel B, et al. Increased cerebral (R)-[^{11}C] PK11195 uptake and glutamate release in a rat model of traumatic brain injury: a longitudinal pilot study. *J Neuroinflammation.* 2011;8:67.
15. Gent YY, Weijers K, Molthoff C, et al. Promising potential of new generation translocator protein tracers providing enhanced contrast of arthritis imaging by positron emission tomography in a rat model of arthritis. *Arthritis Res Ther.* 2014;16:R70.
16. Gent YY, Voskuyl AE, Kloet RW, et al. Macrophage positron emission tomography imaging as a biomarker for preclinical rheumatoid arthritis: findings of a prospective pilot study. *Arthritis Rheum.* 2012;64:62–66.
17. van der Laken CJ, Elzinga EH, Kropholler MA, et al. Noninvasive imaging of macrophages in rheumatoid synovitis using ^{11}C-(R)-PK11195 and positronCemission tomography. *Arthritis Rheum.* 2008;58:3350–3355.
18. Yui J, Maeda J, Kumata K, et al. ^{18}F-FEAC and ^{18}F-FEDAC: PET of the monkey brain and imaging of translocator protein (18 kDa) in the infarcted rat brain. *J Nucl Med.* 2010;51:1301–1309.
19. Yanamoto K, Kumata K, Yamasaki T, et al. [^{18}F]FEAC and [^{18}F]FEDAC: two novel positron emission tomography ligands for peripheral-type benzodiazepine receptor in the brain. *Bioorg Med Chem Lett.* 2009;19:1707–1710.
20. Hatori A, Yui J, Yamasaki T, et al. PET imaging of lung inflammation with [^{18}F] FEDAC, a radioligand for translocator protein (18 kDa). *PLoS One.* 2012;7:e45065.
21. Yanamoto K, Kumata K, Fujinaga M, et al. In vivo imaging and quantitative analysis of TSPO in rat peripheral tissues using small-animal PET with [^{18}F] FEDAC. *Nucl Med Biol.* 2010;37:853–860.
22. Mosser DM, Zhang X. Activation of murine macrophages. *Curr Protoc Immunol.* 2008;chapter 14:unit 14.2.
23. Brand DD, Latham KA, Rosloniec EF. Collagen-induced arthritis. *Nat Protoc.* 2007;2:1269–1275.
24. Wang M, Wang X, Zhao L, et al. Macroglia-microglia interactions via TSPO signaling regulates microglial activation in the mouse retina. *J Neurosci.* 2014; 34:3793–3806.
25. Karlstetter M, Nothdurfter C, Aslanidis A, et al. Translocator protein (18 kDa) (TSPO) is expressed in reactive retinal microglia and modulates microglial inflammation and phagocytosis. *J Neuroinflammation.* 2014;11:3.
26. Irmler IM, Gebhardt P, Hoffmann B, et al. ^{18}F-fluoride positron emission tomography/computed tomography for noninvasive in vivo quantification of pathophysiological bone metabolism in experimental murine arthritis. *Arthritis Res Ther.* 2014;16:R155.
27. Briard E, Zoghbi SS, Imaizumi M, et al. Synthesis and evaluation in monkey of two sensitive ^{11}C-labeled aryloxyanilide ligands for imaging brain peripheral benzodiazepine receptors in vivo. *J Med Chem.* 2008;51:17–30.